JOURNAL OF AIRCRAFT
Vol. 29, No. 4, July–Aug. 1992

Noise of Two High-Speed Model Counter-Rotation Propellers at Takeoff/Approach Conditions

Richard P. Woodward*
NASA Lewis Research Center, Cleveland, Ohio 44135

Modern high-performance turboprop aircraft offer the promise of considerable fuel savings while still allowing for a cruise speed similar to that of current turbofan aircraft. However, there is considerable concern about the potential noise generated by such aircraft, which includes both in-flight cabin noise and community noise during takeoff and landing. This paper presents acoustic results for two model counter-rotation propellers which were tested in the NASA Lewis 9- × 15-ft Anechoic Wind Tunnel. The propellers had a common forward rotor, but the diameter of the aft rotor of the second propeller was reduced in an effort to reduce its interaction with the forward rotor tip vortex. The propellers were tested at Mach 0.20, which is representative of takeoff/approach operation. Acoustic results are presented for these propellers which show the effect of rotor spacing, reduced aft rotor diameter, operation at angle-of-attack, blade loading, and blade number. Limited aerodynamic results are also presented to establish the propeller operating conditions.

Introduction

MODERN high-performance turboprop aircraft offer the promise of considerable fuel savings while still allowing for a cruise speed similar to that of current turbofan aircraft. Advanced counter-rotation propellers may offer from 8–10% additional fuel savings over similar single rotation propellers at cruise conditions.[1] However, there is considerable concern about the potential noise generated by such aircraft, which includes both in-flight cabin noise and community noise during takeoff and landing.

This article presents acoustic results for two model counter-rotation propellers which were tested in the NASA Lewis 9- × 15-ft Anechoic Wind Tunnel. The test results are for a tunnel Mach number of 0.20, which is representative of takeoff/approach operation. The first test propeller,[2] designated F7/A7, was primarily tested with 11 forward and 9 aft blades (11 + 9 configuration), although data are included for an 8 + 8 configuration for comparison. The second propeller,[3] designated F7/A3 was only tested in the 11 + 9 blade configuration. The forward F7 rotor was common to both propellers. The aft A7 rotor had almost the same diameter as did the forward F7 rotor (Table 1); however, the aft A3 rotor diameter was reduced by about 15% to minimize interaction with the forward rotor tip vortex,[4–6] and thus reduce its interaction tone levels. Forward rotor tip flow calculations[5,6] suggest that much of the forward rotor tip vortex will be missed by the reduced-diameter aft rotor. However, no actual flow measurements were made in this study.

These propellers were tested at three rotor-rotor axial spacings and at propeller axis angles-of-attack up to ±16 deg. The propellers were primarily tested at two blade setting angles to investigate loading effects. Acoustic data for rotor-alone and interaction tones are presented for the two propellers showing the effects of angle-of-attack operation, blade loading, and reduced aft rotor diameter on the sideline and circumferential propeller tone sound pressure level (SPL) directivities. Results for the F7/A7 propeller with two forward rotor blade numbers (11 and 8) are included to show the acoustic effects of this parameter. Limited aerodynamic results are included to establish propeller operating conditions. Data in this paper are for the uninstalled, or baseline configuration.

Table 1 Propeller design characteristics

	Cruise conditions
F7/A7 Propeller	
Number of blades[a]	11/9
Design cruise Mach number	0.72
Nominal diameter, cm (in.)	62.2(24.5)/60.7(23.9)
Nominal design cruise tip speed, m/s (ft/s)	238(780)
Nominal design advance ratio	2.82
Hub-to-tip ratio	0.42
Geometric tip sweep, deg	34/31
Activity factor	150/150
Design power coefficient based on annulus area	4.16
F7/A3 Propeller	
Number of blades	11/9
Design cruise Mach number	0.72
Nominal diameter, cm (in.)	62.2(24.5)/53.1 (20.9)
Nominal design cruise tip speed, m/s (ft/s)	238(780)/203(665)
Nominal design advance ratio	2.82/3.32
Hub-to-tip ratio	0.42/0.49
Geometric tip sweep, deg	34/22
Activity factor	150/243
Design power coefficient based on annulus area	4.16

[a]Forward propeller/aft propeller.

Apparatus

Anechoic Wind Tunnel

The NASA Lewis 9- × 15-ft Anechoic Wind Tunnel is located in the low-speed return leg of the supersonic 8- × 6-ft Wind Tunnel. The maximum airflow velocity in the test section is slightly over Mach 0.20, which provides a takeoff/approach test environment. The tunnel acoustic treatment provides anechoic conditions down to a frequency of 250 Hz, which is lower than the range of the test propeller fundamental tones.

Presented in parts as Paper 87-2657 at the AIAA 11th Aeroacoustics Conference, Sunnyvale, CA, Oct. 19–21, 1987, and Paper 88-0263 at the AIAA 26th Aerospace Sciences Meeting, Reno, NV, Jan. 11–14, 1988; received April 19, 1990; revision received Sept. 3, 1991; accepted for publication Sept. 5, 1991.

*Aerospace Engineer. Member AIAA.

Acoustic instrumentation in the 9- × 15- ft Tunnel consisted of two remote-controlled acoustic probes, a "track" probe and a "polar" probe. Figure 1 shows a model propeller with acoustic instrumentation installed in the Anechoic Wind Tunnel. The probes were instrumented with 0.64 cm (0.25 in.) condenser microphones. The track probe, which featured two microphones, was fixed to the tunnel floor. The polar probe was attached to the downstream propeller housing. Data presented in this paper are for the polar microphone probe.

The polar microphone probe had the capability to survey much of the propeller noise field. Figure 2 is a sketch of the polar microphone probe installed on the propeller housing. The probe could acquire sideline acoustic surveys extending from 45 deg forward of the aft propeller plane to 45 deg aft of the plane. Circumferential surveys could be made over a 240 deg range at any sideline location (Θ), being limited by support hardware interference. However, it was possible to generate 360 deg directivities by combining the results for corresponding positive and negative angles-of-attack (α). The polar probe microphone was located 61 cm (24 in.) from the propeller axis of rotation (approximately one propeller diameter). Figure 3(a) shows the angular convention which was used to identify circumferential angles for the polar probe circumferential surveys. The track microphone probe was fixed at the $\phi = 180$ deg circumferential location, which corresponds to "below a hypothetical aircraft." Propeller axis angle-of-attack was achieved by rotating the propeller in the horizontal plane, with positive "α" values being away from the track probe (Fig. 3b).

Test Propellers

Two model counter-rotation propellers were tested in this study (Fig. 4). The forward rotor (designated F7) was common to both propellers. Table 1 presents selected design parameters for the two propellers. Table 2 presents selected aerodynamic results for the two propellers at the Mach 0.20 test conditions. The F7/A7 propeller was also tested in the 8 + 8 blade configuration, with aerodynamic results presented in Ref. 7. The propeller installation in the 9- × 15-ft wind tunnel was powered by two independent air turbine drives, allowing operation of forward and aft rotors at different speeds. The two rotors were operated at about 100 rpm difference to relieve the higher test rig stress experienced with nearly equal rotor speeds.

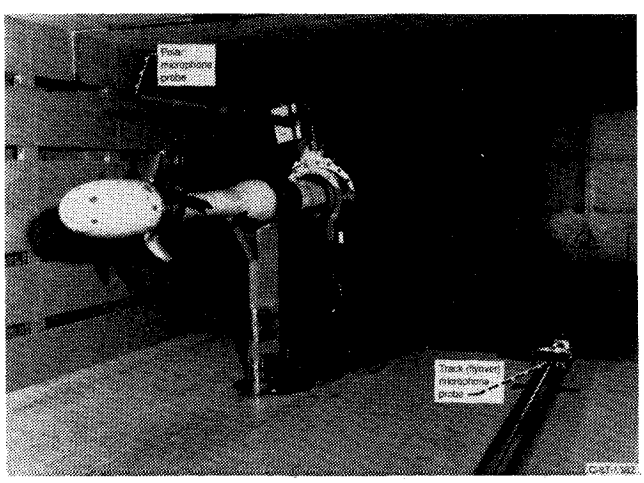

Fig. 1 Photograph of the counter-rotation turboprop model in the 9- × 15-ft Anechoic Wind Tunnel.

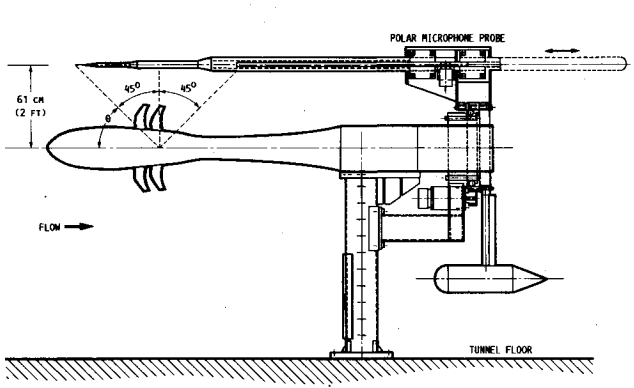

Fig. 2 Sketch of the turboprop model and polar microphone probe.

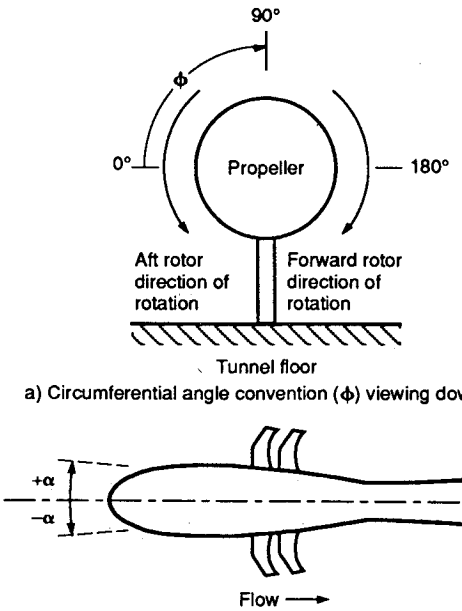

Fig. 3 Angular conventions for circumferential position and propeller axis angle-of-attack.

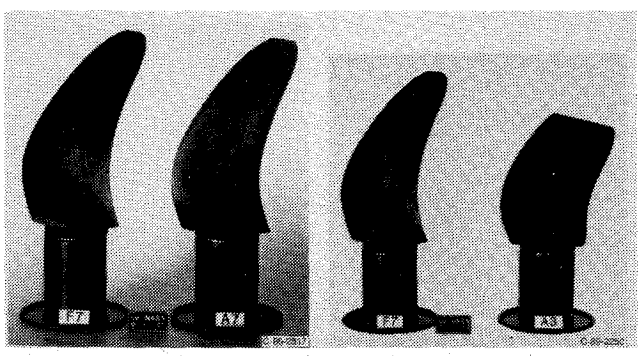

a) F7/A7 **b) F7/A3, reduced diameter aft propeller**

Fig. 4 Propeller configurations.

The model propellers were operated at propeller axis angle-of-attack up to ±16 deg. The propellers were tested with forward rotor blade setting angles of 36.4 deg (measured at $\frac{3}{4}$ radius) at three rotor axial spacings, and at a higher loading 41.1 deg blade setting angle at the maximum spacing (Table 2). The aft rotor blade setting angles were adjusted for each propeller to obtain an equal forward/aft torque split. The higher blade setting angle (and blade loading) of 41.1 deg for the forward rotor is more typical of what would be used on a full-scale counter-rotation propeller at takeoff conditions. The smaller-diameter A3 aft rotor required a higher blade setting angle (and consequently higher spanwise loading) to achieve torque (and thrust) output comparable to that of the A7 rotor.

Aerodynamic Results

Figure 5 is a propeller operating map of the total power coefficient (based on the forward rotor), $PQAT_1$, as a function

Table 2 Selected aerodynamic results

Speed, %	Spacing,[a] cm, in.	Blade angle, deg	PQAT$_1$[b]	J_1	J_2	rpm$_1$	rpm$_2$	Thrust$_1$, N	Thrust$_2$, N	Torque split, τ_1/τ_2
F7/A7 Propeller, 11 + 9										
85	15.0(5.9)	41.1/39.4	3.534	0.923	0.942	7201	7261	NA	1464	1.01
90	15.0(5.9)	41.1/39.4	3.500	0.874	0.892	7614	7674	1833	1686	0.97
90	8.5(3.3)	36.4/36.5	2.408	0.870	0.889	7649	7703	1416	1349	0.89
90	10.6(4.2)	36.4/36.5	2.448	0.866	0.885	7637	7693	1452	1342	0.90
90	15.0(5.9)	36.4/36.5	2.454	0.864	0.882	7633	7695	1517	1277	0.97
F7/A3 Propeller, 11 + 9										
85	15.0(5.9)	41.1/46.4	3.530	0.992	1.076	7219	7265	1600	1411	0.96
90	15.0(5.9)	41.1/46.4	3.671	0.862	1.006	7655	7708	1844	1663	0.93
90	8.5(3.3)	36.4/43.5	2.455	0.868	1.013	7647	7707	1425	1256	0.88
90	10.6(4.2)	36.4/43.5	2.477	0.863	1.007	7633	7691	1450	1250	0.88
90	15.0(5.9)	36.4/43.5	2.527	0.864	1.008	7637	7693	1495	1274	0.93

0-deg Angle of attack, $M_\infty = 0.2$
Subscripts: 1 denotes forward rotor; 2 denotes aft rotor.
[a]Spacing is defined as axial distance between rotor pitch change axis.
[b]PQAT is defined as power/(ρ)(rev/s)$^3(D)^3$(annulus area) where ρ is the local air density, and D is the propeller diameter. PQAT is based on forward rotor conditions.

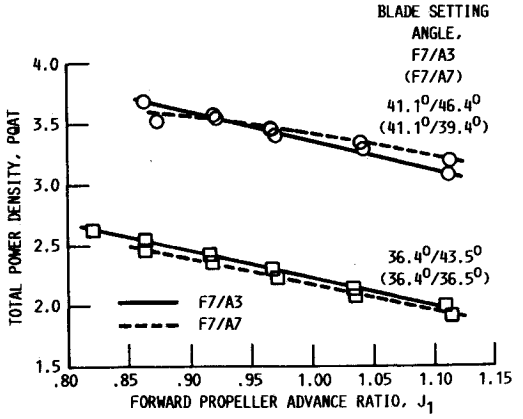

Fig. 5 Propeller operating map for maximum rotor spacing comparing F7/A7 and F7/A3 propellers (α = 9 deg, M_∞ = 0.2).

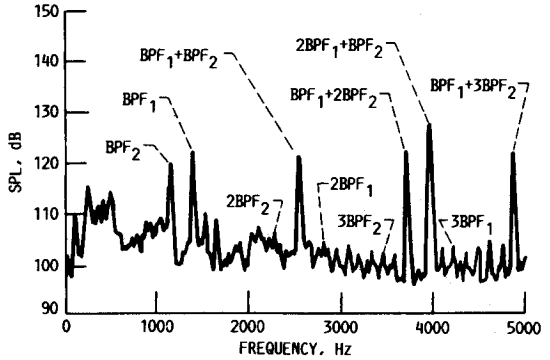

Fig. 6 Typical SPL spectrum for the F7/A3 11 + 9 turboprop. Data is for the polar microphone at 105-deg sideline angle (90% speed, β_1/β_2 = 36.4 deg/43.5 deg, intermediate rotor spacing, α = 0 deg, M_∞ = 0.2).

of the forward propeller advance ratio, J_1. (PQAT$_1$ is defined in Table 2.) The results in Fig. 5 are for the rotors at maximum spacing.

Acoustic Results

Sideline and circumferential sound pressure level (SPL) directivities were taken with the polar microphone probe. Data will be presented which show the acoustic effects of propeller axis angle-of-attack, blade loading, rotor spacing, and blade number. All data were analyzed at a 16-Hz bandwidth.

The acoustic spectra for counter-rotation propellers may be quite complex, consisting of both rotor-alone tone harmonics for each propeller and an array of interaction tones. Figure 6 presents a typical SPL spectrum for the F7/A3 propeller. Rotor-alone tones typically show a maximum level near the propeller plane, while the interaction tones are often higher at forward and aft angles. The spectrum of Fig. 6 is for 105 deg from the upstream propeller axis (relative to the aft propeller plane) along the 61 cm (24 in.) sideline. The fundamental rotor-alone tones (BPF$_1$ and BPF$_2$) are clearly seen in the spectrum, but the higher-order rotor-alone tones are essentially buried in the broadband. Interaction tones (such as BPF$_1$ + BPF$_2$) dominate the spectrum at higher frequencies.

Sideline Directivities at Angle-of-Attack

Rotor-alone tone levels are strongly affected by propeller axis angle-of-attack.[2,3,8] These tone level changes are associated with local changes in the propeller blade angle-of-attack, with higher blade loading producing higher noise. Propeller tone noise typically propagates normal to the advancing blade. Thus, tone level increases associated with local blade loading increases would be observed approximately 90 deg circumferentially ahead of the region of increased blade loading.

Figure 7 presents F7/A7 sideline directivities "below the aircraft" (ϕ = 180 deg, 61 cm (24 in.) sideline distance). Positive angles of attack correspond to the propeller axis in a "climb" orientation (positive α, see Fig. 3). Figures 7a and 7b show the rotor-alone (BPF$_1$ and BPF$_2$) tone directivities. The forward rotor-alone tone varies by about 27 dB over the ±16 deg range of angles-of-attack. The corresponding aft rotor-alone tone varies by over 20 dB. The directivity trends for the two representative interaction tone orders (BPF$_1$ + BPF$_2$ and 2BPF$_1$ + BPF$_2$) with propeller axis angle-of-attack are much less defined, indicating that propeller axis angle-of-attack is not a strong influence for these tone orders in the aft rotor plane.

Figure 8 shows the F7/A7 SPL at three sideline locations at ϕ = 180 deg. Results are shown for sideline angles of Θ = 60, 90, and 120 deg relative to the aft rotor plane. These graphs show that the rotor-alone tones vary directly with angle-of-attack, while the levels of the interaction tones at this circumferential location are less affected by this parameter.

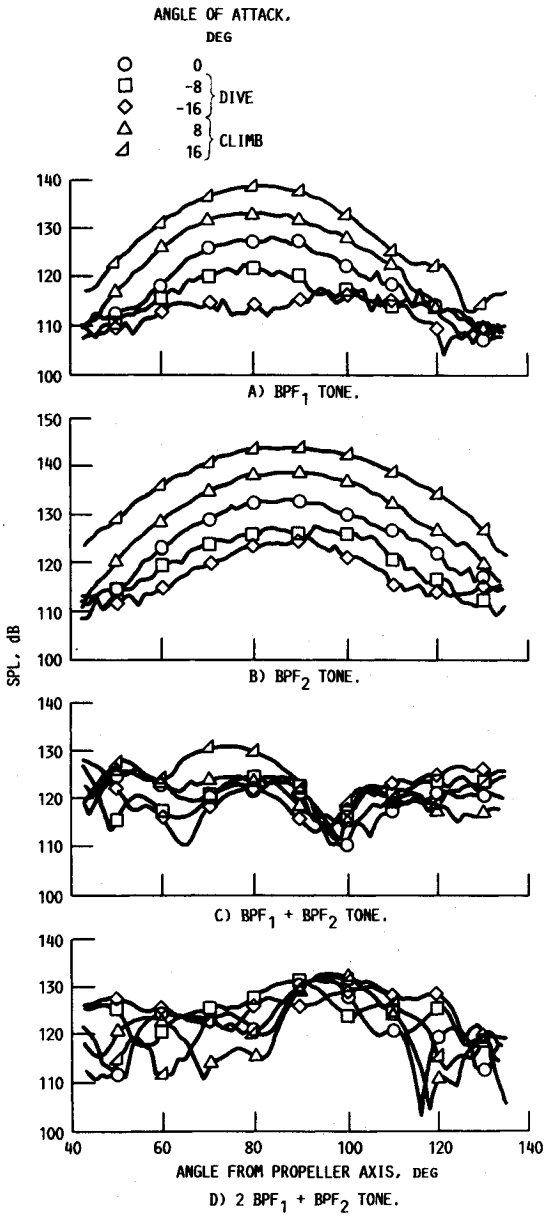

Fig. 7 F7/A7 tone directivity along a 61-cm (24-in.) sideline for several propeller axis angles-of-attack (90% speed, β_1/β_2 = 36.4 deg/36.5 deg, intermediate rotor spacing, ϕ = 180 deg, Θ = 90 deg, M_∞ = 0.2).

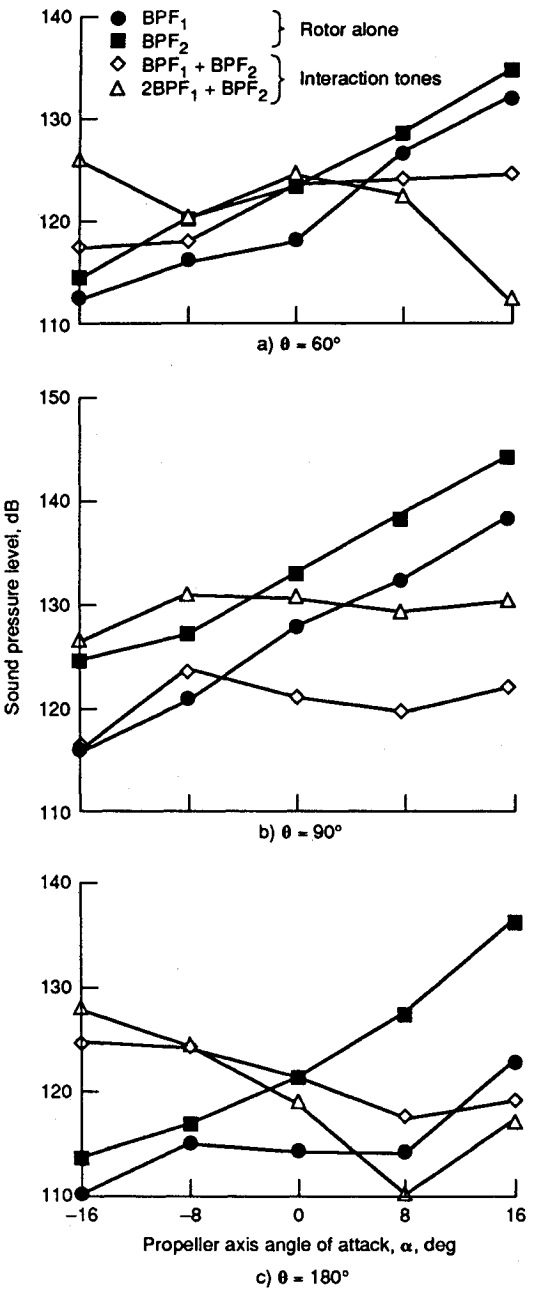

Fig. 8 F7/A7 tone sound pressure level "below the aircraft" (90% speed, β_1/β_2 = 36.4 deg/36.5 deg, intermediate rotor spacing, ϕ = 180 deg, M_∞ = 0.2).

The reader should note that the interaction tone levels often change rapidly with sideline angle (Fig. 7). Consequently, small changes in the sideline angle measuring point can substantially affect the interaction tone levels in Fig. 8.

The rotor-alone tone for the aft A7 rotor is typically about 5 dB higher than that for the forward F7 rotor in the region of Θ = 90 deg (Fig. 8b). Both rotors are of about the same diameter, and are operating at essentially the same tip speed and blade setting angles. This tone level difference may be explained by the difference in blade number for the two propellers.

Reference 9 presents a discussion on how parameters such as blade number and tip speed may affect rotor-alone tone level. This reference gives the following Gutin-type analysis for an estimate of the strength of the "m" harmonic for a propeller as

$$mBJ_{mB}(0.8M_t mB \sin\theta)$$

where m is the order of the harmonic, B is the number of blades, M_t is the blade tip rotational Mach number, and $J_n(x)$ is a Bessel function of the first kind of order n and argument x. Solving this expression for the fundamental tone, m = 1, for the 9- and 11-blade rotors at 90% speed lead to a predicted 4.5-dB maximum sideline noise increase for the 9-bladed propeller, which is in excellent agreement with the observed difference in tone level in Fig. 8b.

Circumferential Directivities at Angle-of-Attack

Figure 9 shows circumferential directivities in the aft propeller plane (Θ = 90 deg) for 8-deg angle-of-attack operation (aircraft climb condition as seen "below the aircraft," ϕ = 180 deg). The results of Fig. 9 are consistent with the sideline results of Fig. 7. The dashed curve shows the forward rotor BPF sound pressure level at 0-deg angle-of-attack (essentially no change with circumferential position). The maximum rotor-alone tone levels occur "below the aircraft" at about ϕ = 200 deg. However, the interaction tone ($2BPF_1 + BPF_2$) shows a minimum at ϕ = 180 deg and a maximum value slightly above the horizontal plane at ϕ = 280 deg. The rotor-alone tones vary circumferentially by almost 30 dB, while the

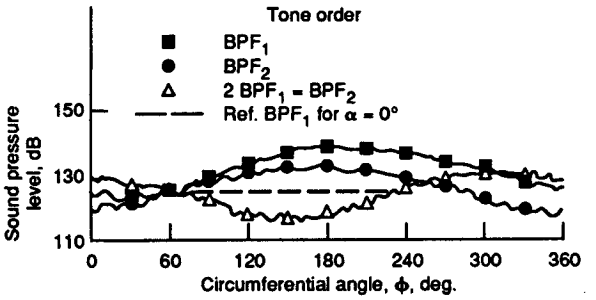

Fig. 9 F7/A7 circumferential directivity in the aft propeller plane (90% speed, β_1/β_2 = 36.4 deg/ 36.5 deg, intermediate rotor spacing, α = 8 deg, Θ = 90 deg, M_∞ = 0.2).

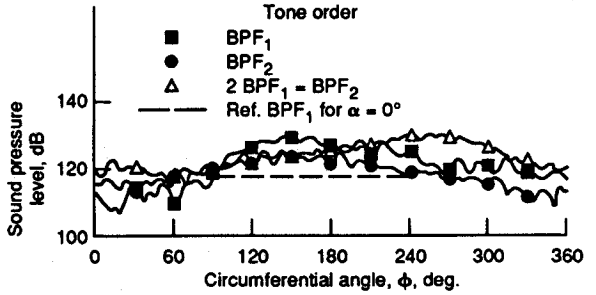

Fig. 10 F7/A7 circumferential directivity (90% speed, β_1/β_2 = 36.4 deg/36.5 deg, intermediate rotor spacing, α = 8 deg, Θ = 60 deg, M_∞ = 0.2).

interaction tone shows about a 16-dB circumferential variation.

The peak level for the interaction tone in Fig. 9 occurs about 90 deg circumferentially from the location of the peak rotor-alone tone. This is consistent with the concept that the interaction tone is generated at the aft rotor, and the circumferential delay in interaction tone response corresponds to the swirl in the forward rotor exit flow. As expected (although not shown here) the circumferential delay in the interaction tone response is also a function of the rotor-rotor separation distance.[3]

Figure 10 shows the circumferential directivities for the first order rotor-alone tones and the $2BPF_1 + BPF_2$ interaction tone at α = 8 deg, and an upstream sideline location of Θ = 60 deg. These results are similar to those at the aft propeller plane (Fig. 9) in terms of circumferential directivity; however, the sound pressure levels are somewhat lower. Although not shown, similar results were observed at the higher, α = 16 deg, propeller axis angle-of-attack.

Effects of Blade Loading

The F7/A7 and F7/A3 propellers were tested at two blade loadings, which were accomplished by different blade setting angles. The more highly loaded case is thought to be more representative of full-scale operation. Figures 11 and 12 show the SPL directivities for two blade loadings for the F7/A3 propeller. Similar acoustic data trends with loading were observed for the F7/A7 propeller. These results are for the polar microphone probe with the propeller at 90% design speed.

The sideline directivities of the rotor-alone tones (Figs. 11a and 11b) typically show about a 5-dB increase with the higher loading. There is no change in the directivity shape. The first interaction tone, $BPF_1 + BPF_2$ (Fig. 11c) is even more sensitive to loading. Higher loading is seen to greatly increase upstream noise levels, showing an increase of 15 dB near Θ = 60 deg. This higher blade loading is likely associated with larger wakes, and hence, increased interaction noise. Also, the minimum noise "trough" moves somewhat forward with higher loading. The results for the $2BPF_1 + BPF_2$ tone likewise show a noise increase with loading.

Figure 12 shows the circumferential directivity results at the aft propeller plane (Θ = 90 deg) for 16-deg propeller axis

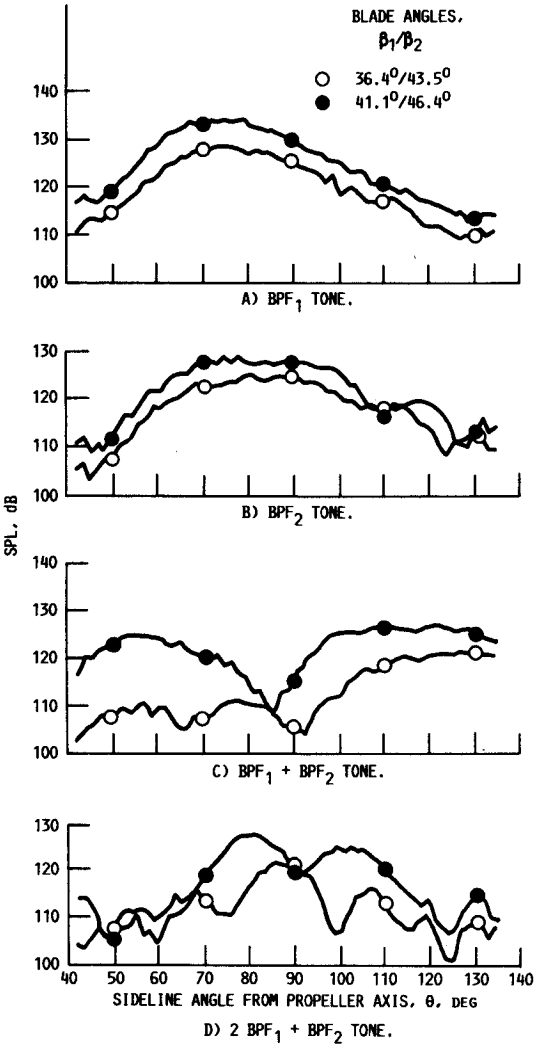

Fig. 11 Effect of F7/A3 blade loading on sideline directivity (61-cm (24-in.) sideline, 90% speed, maximum rotor spacing, α = 0 deg, aft propeller plane at Θ = 90 deg, M_∞ = 0.2).

angle-of-attack. The rotor-alone tones (Fig. 12a) show no angular change in the directivity shape with loading. There is about a 5-dB tone level increase with loading at most angles except near ϕ = 200 deg, where the tone increase with loading is somewhat less. The dashed lines on Fig. 12a show reference levels for the forward rotor BPF at 0-deg angle-of-attack for both loadings (corresponding to the levels at 90 deg in Fig. 11a).

The results for the first two interaction tones with loading (Fig. 12b) are more complicated. The $BPF_1 + BPF_2$ tone level is 3 to 5 dB higher with increased loading in the ϕ = 50–230 deg region. The smaller SPL variation with loading for the $BPF_1 + BPF_2$ tone may be because this circumferential survey was performed in the aft propeller plane where the SPL for this tone is minimum (Fig. 11c). The $2BPF_1 + BPF_2$ interaction tone is more sensitive to loading, showing as much as a 10-dB increase near 180 deg. However, the increase with loading is only 2 dB near ϕ = 270 deg for this tone.

Effects of Rotor-Rotor Spacing

Blade row spacing is expected to have a significant effect on the interaction tone levels, which are primarily generated from interaction with the forward rotor viscous wakes and tip vortices. Of these two mechanisms, the decay of the tip vortices is slower with downstream distance. The reduced diameter A3 propeller was designed to reduce interaction with these vortices, leaving the more rapidly decaying viscous wakes as the main interaction tone generating mechanism. (As previously mentioned, there were no actual flow measurements

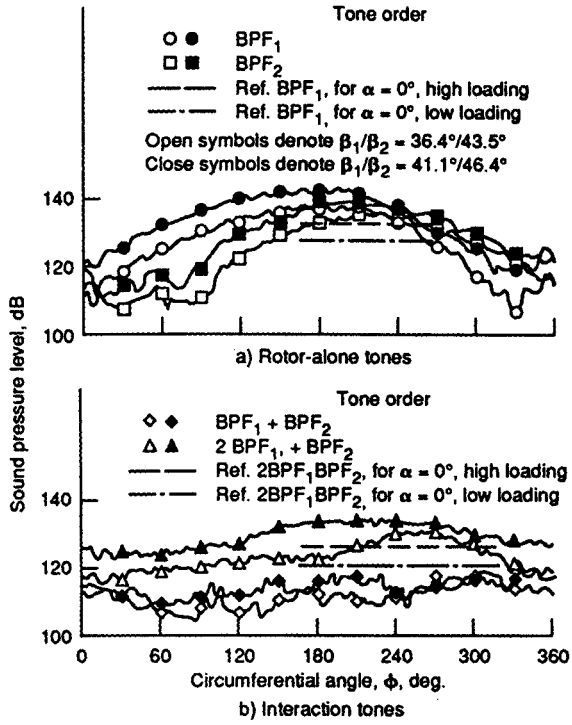

Fig. 12 Effect of F7/A3 blade loading on circumferential directivity in the aft propeller plane (90% speed, maximum rotor spacing, α = 16 deg, Θ = 90 deg, M_∞ = 0.2).

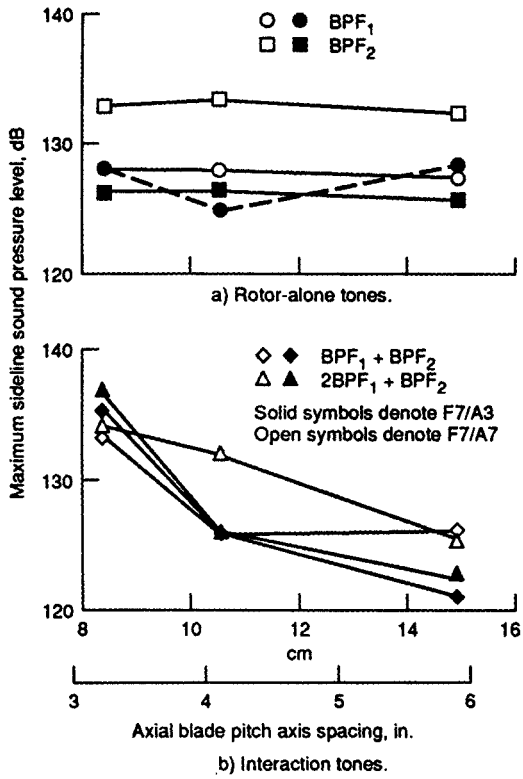

Fig. 13 Comparison of F7/A7 and F7/A3 blade row spacing effects (61-cm (24-in.) sideline, 90% speed, F7/A7: β_1/β_2 = 36.4 deg/36.5 deg, F7/A3: β_1/β_2 = 36.4 deg/43.5 deg, α = 0 deg, ϕ = 180 deg, M_∞ = 0.2).

made during this study to quantify the character of the upstream rotor tip vortex.) Figure 13 summarizes the effect of rotor spacing for the two propellers. These results show the maximum observed sideline tone levels for the polar probe with the propellers at 0-deg angle-of-attack. The propellers were operated at the lower loading blade setting angles and at the three rotor spacing values described in Table 2.

The rotor-alone tones for the two propellers show essentially no level change with rotor spacing (Fig. 13a) with the possible exception of the lower tone level observed for the forward rotor of the F7/A3 propeller at the intermediate spacing. However, corresponding results at the further 137 cm (54 in.) sideline of the track probe did not show any significant change in rotor-alone tone level with rotor spacing. The tone level for the forward F7 rotor (common to both propellers) is the same for both propellers at the "minimum" and "maximum" spacings. The tone level for the aft A7 rotor is about 7 dB higher than that for the aft A3 rotor. Again referring to the Gutin-type analysis which was outlined earlier in this discussion, it is seen that the propeller tone level is a function of both blade number and tip speed. Both the aft A7 and A3 rotors have the same blade number; however, the A3 rotor operates at a lower tip speed for the same rotational speed. Applying this analysis to the two aft rotors yields a predicted 10.7-dB rotor-alone tone level difference based on tip speed ratio. Although this expression was formulated for change in the same propeller, the predicted SPL change is close to what was observed for the two aft rotors.

The plot of interaction level with spacing (Fig. 13b) shows that the interaction tones for the F7/A3 propeller decrease more rapidly with increased spacing than do the corresponding tones for the F7/A7 propeller. Also, the F7/A3 interaction

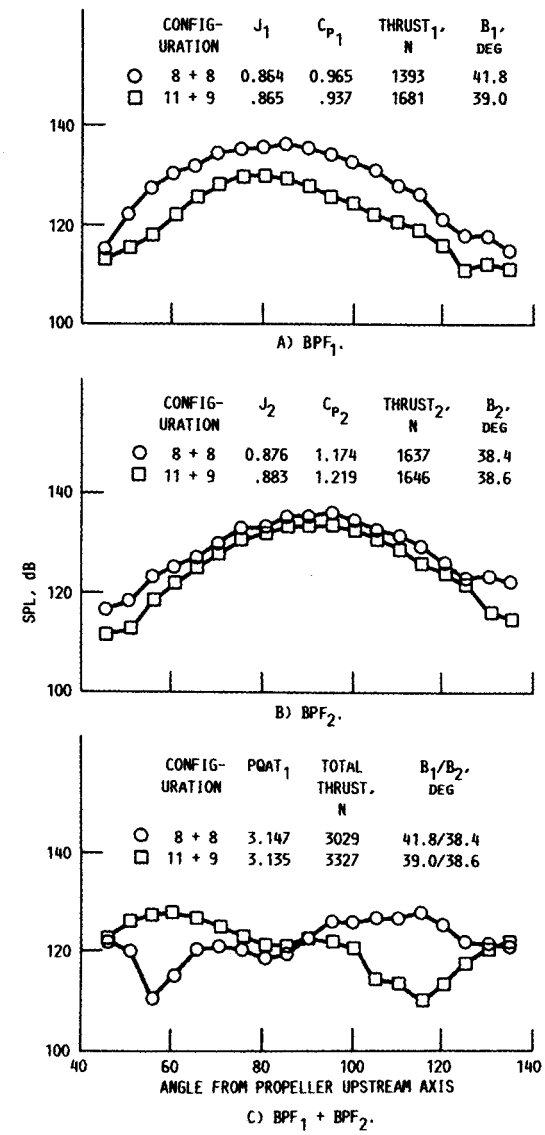

Fig. 14 Comparison of F7/A7 tone noise along a 61-cm (24-in.) sideline for the 8 + 8 and 11 + 9 configurations (90% speed, rpm_1/rpm_2 = 7650/7750, aft propeller plane at Θ = 90 deg, M_∞ = 0.2).

tones are higher at the minimum spacing, but lower at the maximum spacing. The measured rates of decrease in tone level with spacing are consistent with the assumption that the A3 rotor is responding primarily to the upstream viscous wake, which decays more rapidly with distance than does the tip vortex. Also, the higher tone levels of the A3 rotor at the minimum spacing may relate to the higher spanwise loading of that rotor (higher blade setting angle to achieve performance similar to that of A7), and consequently, greater acoustic response to the upstream viscous wake.

Effects of Blade Number

The F7/A7 propeller was first run in the 8 + 8 blade configuration. Mismatching the blade numbers allowed for easier acoustic analysis as well as providing data on the acoustic effects of loading per blade. Figure 14 compares the sideline directivities for the two configurations at 0-deg angle-of-attack. Data are presented for two closely matched blade angle configurations with respect to total stage thrust.

Figure 14a compares the forward rotor BPF tone directivities for the two configurations. There is a significant difference in blade numbers (8 and 11). The 11-blade rotor produced the higher thrust (1681 N vs 1393 N) at a lower blade setting angle (39 deg vs 41 deg). The results of Fig. 14a show that the rotor-alone tone SPL for the eight-blade rotor was as much as 8 dB higher. This relates to the higher loading per blade of the eight-blade rotor and clearly shows the acoustic advantage of increased blade number.

The aft propeller rotor-alone tone level for the eight-blade rotor (Fig. 14b) is about 2 dB higher than that for the nine-blade rotor. Here the blade numbers (8 and 9), blade setting angles, and propeller thrust are more nearly matched.

The $BPF_1 + BPF_2$ interaction tone, Fig. 14c, shows no clear noise advantage for higher blade numbers. Different modal generation mechanisms for the two configurations result in higher upstream tone levels for the 9 + 11 blade configuration, and higher downstream tone levels for the 8 + 8 blade configuration.

The Gutin-type analysis of Ref. 9 may again be applied to help understand the rotor-alone tone differences between the 8 + 8 and 11 + 9 blade propellers. Solving this expression for the fundamental tone, $m = 1$, for the 8- and 11-blade forward rotors leads to an expected 6.7-dB maximum sideline tone level increase for the eight-blade rotor, which is in good agreement with the observed 8-dB tone level increase (Fig. 14a).

Similarly, solving this expression for the fundamental tone for the eight- and nine-blade aft rotor leads to an expected 2.2-dB difference in maximum sideline noise levels. Again, this prediction is in excellent agreement with the experimental results of Fig. 14b.

Summary of Results

Two advanced-model counter-rotation turboprops were acoustically tested in the NASA Lewis 9- × 15-ft Anechoic Wind Tunnel at a simulated takeoff/landing speed of Mach 0.20. The propellers were tested over a range of rotor axial spacings and propeller axis angles-of-attack. Data were taken at two blade setting angles to investigate blade loading effects. The following significant results were observed in this study:

1) The first-order rotor-alone tones (BPF_1 and BPF_2) dominate the sideline directivities near the rotor plane. The interaction tones ($BPF_1 + BPF_2$, etc.) show high levels throughout the sideline directivities, with the highest levels often observed toward the propeller axis.

2) The sideline noise levels for the rotor-alone tones are strongly influenced by propeller axis angle-of-attack. The forward rotor BPF tone increases by about 27 dB over the range of ±16 deg, with slightly lower increases observed for the aft rotor. Interaction tone level showed significantly less sensitivity to this parameter.

3) A Gutin-type analysis yielded a first approximation of relative rotor-alone tone levels based on tip speed and blade number. This procedure accurately predicted the 10-dB tone level reduction observed for the aft A3 rotor relative to the A7 rotor due to reduced tip speed with the same blade number. This procedure also accurately predicted observed rotor-alone tone level differences between the 11 + 9 and 8 + 8 blade configurations of the F7/A7 propeller when operated at the same tip speeds.

4) The interaction tone levels for the F7/A3 propeller decrease more rapidly with blade row spacing than do the corresponding results for the F7/A7 propeller. This result suggests that the interaction tones for the F7/A3 propeller are primarily controlled by the forward propeller viscous wake. The rotor-alone tone levels were not affected by rotor-rotor spacing.

5) Increased blade loading (i.e., higher blade setting angles at the same rotational speed) increases the rotor-alone tone levels, but does not affect their angular directivity. However, the first interaction tone ($BPF_1 + BPF_2$) shows a substantial noise level increase with loading accompanied by a shift in the maximum tone level toward the upstream axis.

References

[1]Mikkelson, D. C., Mitchell, G. A., and Bober, L. J., "Summary of Recent NASA Propeller Research," Aerodynamics and Acoustics of Propellers, AGARD CP-366, AGARD, Neuilly-Sur-Seine, France, 1985, pp. 12-1 to 12-24. (also, NASA TM-83733, 1984).

[2]Woodward, R. P., "Noise of a Model High Speed Counterrotation Propeller at Simulated Takeoff/Approach Conditions (F7/A7)," AIAA Paper 87-2657, NASA TM-100206, 1987.

[3]Woodward, R. P., and Gordon, E. B., "Noise of a Model Counterrotation Propeller With Reduced Aft Rotor Diameter at Simulated Takeoff/Approach Conditions (F7/A3)," AIAA Paper 88-0263, NASA TM-100254, 1988.

[4]Dittmar, J. H., "Some Design Philosophy for Reducing the Community Noise of Advanced Counter-Rotation Propellers," NASA TM-87099, 1985.

[5]Majjigi, R. K., Uenishi, K., and Gliebe, P. R., "An Investigation of Counterrotating Tip Vortex Interaction," NASA CR-185135, 1989.

[6]Hoff, G. E., et al., "Experimental Performance of Acoustic Investigation of Modern, Counterrotating Blade Concepts," NASA CR-185158, 1990.

[7]Sullivan, T. J., "Aerodynamic Performance of a Scale-Model, Counter-Rotating Unducted Fan," *Advanced Technology for Aero Gas Turbine Components*, AGARD CP-421, Sept. 1987, p. 16.

[8]Dittmar, J. H., "Cruise Noise of a Counterrotation Propeller at Angle of Attack in Wind Tunnel," NASA TM-88869, 1986.

[9]Richards, E. J., and Mead, D. J., *Noise and Acoustic Fatigue in Aeronautics*, Wiley, New York, 1968, p. 189.